The 21st International Symposium on Transport Phenomena
2-5 November, 2010, Kaohsiung City, Taiwan

PULSATING HEAT PIPE BASED HEAT EXCHANGERS

Sameer Khandekar

Department of Mechanical Engineering
Indian Institute of Technology Kanpur, Kanpur (UP) 208016 India

ABSTRACT

We explore and scrutinize two possible configurations of Pulsating Heat Pipe (PHP) based heat exchangers for process waste heat exchange as well as high heat flux handling needs, respectively. Temperature controlled liquid-liquid non-contact type heat exchangers and heat flux controlled air cooled systems are studied. The experimental thermal performance of these heat exchangers is highlighted under different operating conditions. While fundamental transport modeling of a pulsating heat pipe has not been achieved as yet, we can still model these heat exchanger systems from a global perspective. The temperature controlled PHP system is effectively modeled by conventional heat exchanger analysis techniques, i.e., the *NTU-ε* method. The heat flux controlled PHP system is modeled by the 'super fin' analogy employing the conventional theory of extended surfaces heat transfer. We present the modeling results with these two techniques and discuss their respective limitations. Before delineating the heat exchanger performance data, we also discuss the essential transport issues which need to be resolved for developing fundamental PHP model.

INTRODUCTION

Innovative heat exchangers are needed to harness or transport energy from various process industry operations. The available thermal energy may often be low-grade and distributed. In addition, high heat flux removal at controlled temperature is needed for power electronics thermal management and transport requirements. The range of Pulsating Heat Pipe (PHP) two-phase systems introduced in the later part of the last century are quite attractive from many aspects [Akachi, 1996; Akachi et al., 1996]. Passive operation, high heat flux handling, ease of manufacture and interesting thermo-fluidic two-phase transport from an academic viewpoint, are some of the striking features of this class of heat pipes [Khandekar, 2004].

Conventional wicked heat pipe heat exchangers have been routinely used for gas-gas heat exchangers for waste heat recovery and air preheating/economizer applications [Vasiliev, 2005]. A PHP heat exchanger has several advantages over conventional heat pipe systems with potentially many applications [Groll and Khandekar, 2003]. Two principal PHP operating modes are possible (i) heat flux controlled and (ii) temperature controlled. Under heat flux controlled mode such structures are inherently capable of handling high heat fluxes ranging from 1 W/cm^2 to over 60 W/cm^2. Under temperature controlled mode, not many experimental studies are available. Before we explore the experimental study of two types of PHP based heat exchangers and their global modeling approach, we briefly review the fundamental two-phase transport processes inside a pulsating heat pipe and its thermal transport behavior.

Transport mechanism of a pulsating heat pipe

The basic structure of a typical pulsating heat pipe consists of meandering capillary tubes having no internal wick structure, as shown in Figure 1-a. The inside diameter of the tube is sufficiently small (critical Bo ~ 1.85) such that surface tension dominates and capillary slug flow is maintained [Khandekar et al. 2003; Zhang and Faghri, 2008]. It can be designed in at least three ways (i) open loop system, (ii) closed loop system and (iii) closed loop with additional flow control check valve(s) as shown in Figure 1-b. The closed loop system allows flow circulation while there is no such possibility in the open loop configuration.

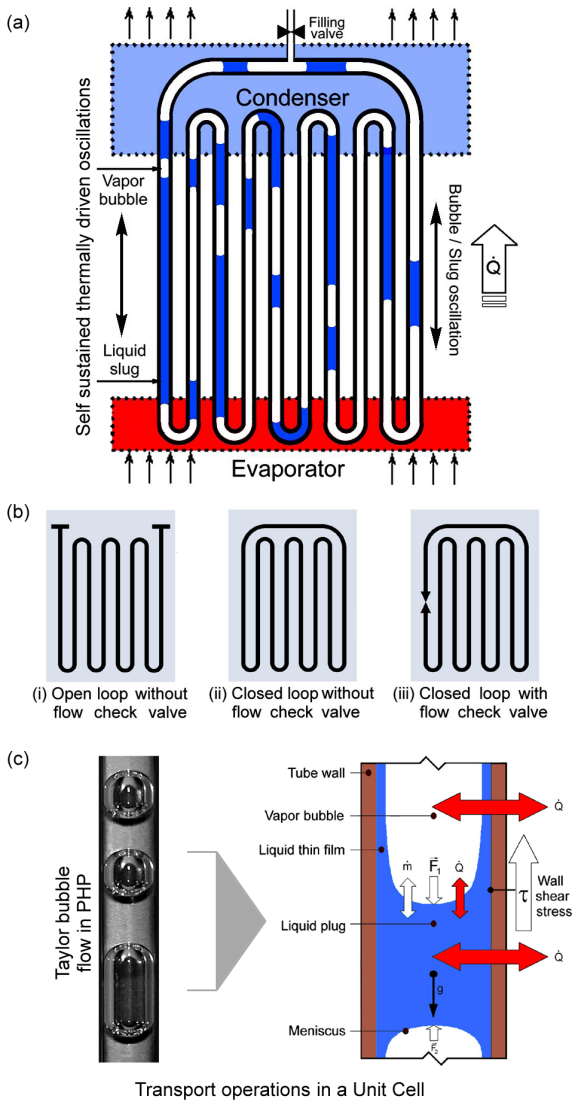

Figure 1. (a) Schematic of a pulsating heat pipe (b) Three possible configurations of a PHP (c) Typical flow pattern in a PHP and the transport operations in a unit cell.

The entire essence of its thermo-mechanical physics lies in the closed (constant volume), two-phase, bubble-liquid slug system, spontaneously formed inside the tube bundle, at the time of filling the device, due to the dominance of surface tension. This tube bundle receives heat at one end and it is cooled at the other end. Temperature gradients give rise to temporal and spatial pressure disturbances due to resulting phase-change phenomena, i.e. generation and growth of bubbles in the evaporator and simultaneous collapse of bubbles in the condenser. The bubbles act as pumping elements, transporting the entrapped liquid slugs in a complex oscillating-translating-vibratory fashion, resulting in self-sustained thermally driven flow oscillations and ensuing highly efficient heat transfer thereof. In addition to the latent heat, considerable amount of sensible heat transfer also occurs in a PHP. While sweeping the evaporator section, a liquid slug accumulates heat, which is eventually transferred to the condenser.

The fundamental transport processes that occur inside the PHP can be understood by looking at Figure 1-c which suggests the various forces, including heat and mass transfer processes acting on a typical liquid-slug vapor-bubble (unit cell) system, as formed inside the PHP. The primary unit-cell processes are:

- The flow pattern in the PHP tubes may be broadly categorized as capillary slug flow. This type of flow is characterized by: (a) the flow pattern is 'generally' axisymmetric, at least in vertical flows (in horizontal flows, there will be some asymmetry depending on the *Bo*, (b) the velocity of large vapor bubbles relative to the liquid slug is somewhat faster [Angeli and Gavriilidis, 2008].
- Due to the capillary dimensions of the PHP tube, a train of liquid slugs and vapor bubbles having menisci on its edges are formed due to surface tension forces. Usually a liquid thin film exists surrounding the vapor bubbles. The angle of contact of the menisci, the liquid thin film stability and its thickness depend on the fluid-solid combination and the selected operating parameters.
- Liquid slugs and vapor bubbles move against the gravity vector, in its direction or at an angle to it, depending on the global PHP orientation and the location of slugs/ bubbles in the up-header or down-header tubes.
- The liquid slugs and vapor bubbles are subjected to pressure force $\vec{F}_1$ and $\vec{F}_2$ from the adjoining slugs/bubbles. These are not only caused due to phase-change mass transfer but also due to capillary forces.
- The liquid slugs and vapor bubbles experience internal viscous dissipation as well as wall shear stress as they move in the PHP tube. Their relative magnitude decides the predominant force to be considered.
- The liquid slugs and vapor bubbles may receive heat, reject heat, or move without any external heat transfer, depending on their location in the evaporator, condenser or the adiabatic section, respectively. Most thermal transport occurs through the thin film and its dynamics plays a crucial role in the overall thermal transport.
- In the evaporator, the liquid slug receives heat which is simultaneously followed by evaporation mass transfer to the adjoining vapor bubbles or breaking up of the liquid slug itself with creation of new bubbles in between as a result of nucleate boiling in the slug flow regime; P_{sat} and T_{sat} thus increase locally. Probability of events frequently places vapor bubbles in direct contact with the internal tube surface of the evaporator. In this case, saturated vapor bubbles receive heat via the liquid thin film surrounding them, which is simultaneously followed up by evaporation mass transfer from the film as well as the adjoining liquid slugs. Heat transfer under such conditions is strongly dependent on local film geometry.
- The above processes in the evaporator are repeated in a reverse direction in the condenser.
- In the adiabatic section, while passing from the evaporator to the condenser, the train of vapor bubbles and liquid slugs is subjected to a series of complex heat and mass transfer processes. Essentially non-equilibrium conditions exist whereby the high pressure, high temperature saturated liquid slugs/vapor bubbles are brought down to low pressure, low temperature saturated conditions existing in the condenser. If ideal adiabatic conditions are maintained, with no axial conduction of heat through the tube wall/ fluid itself, then an inherently irreversible isenthalpic process can accomplish this task. Internal enthalpy balancing in the form of latent heat takes place by evaporation mass transfer from the liquid slugs to the vapor bubbles whereby saturation conditions are always imposed on the system during the bulk transit in the adiabatic section. In real systems, this transit is certainly much more complex with non-equilibrium metastable conditions existing throughout.

It is to be noted that there occurs no 'classical steady state' in PHP operation as far as the internal hydrodynamics is concerned. Instead, pressure waves and pulsations are generated in each of the individual tubes, which interact with each other possibly generating secondary and ternary reflections with perturbations. The self-exited thermally driven oscillations are dependent on many operating variables [Khandekar, 2004].

There are several important and unresolved issues with the present understanding of PHPs [Zhang and Faghri, 2008; Das et al., 2010].

(i) At present there is no comprehensive mathematical model to predict the thermal performance of pulsating heat pipe under a given boundary condition.

(ii) The understanding of heat transfer and pressure drop under self-excited thermally driven oscillating two-phase flow inside capillary tubes is quite unsatisfactory.

(iii) The complete transport phenomena in the unit-cell, remains unresolved.

(iv) Multiple unit-cells, also interact with each other mutually; merger and coalescence of liquid slugs, breakage of Taylor bubbles under the impact of inertia and surface tension, nucleation inside liquid slugs, confined bubble formation, condensation on liquid films, instabilities, surface waves, etc. are additional complexities which makes transport prediction difficult.

In this background, we now explore the global behavior of two types of heat exchangers (a) Temperature controlled (liquid-liquid) module and (b) heat flux controlled air-cooled module. As we will see, in spite of the fact that fundamental level of transport modeling of PHPs has not been achieved till date, global statistical behavior can still be predicted by the approaches proposed in this paper.

TEMPERATURE CONTROLLED MODULE

Experimental set-up

This module was designed for passive heat transfer between two liquids without mixing. The details of the module are shown in Figure 2-a,b. The PHP matrix was made of copper tube (ID 1.8 mm and OD 2.0 mm) and was fabricated with a stainless steel splitter plate in between (256 mm × 146 mm × 8 mm) which had 120 holes (longitudinal pitch = transverse pitch = 12 mm) arranged in staggered mode. U-shaped copper capillary tubes were brazed on both sides of these holes forming a complete and endless closed loop PHP. Height of every loop was 150±1 mm each, on both sides of the splitter plate. Net volume of PHP was measured to be 92±2 ml. Working fluid was ethanol in all tests.

The PHP matrix was assembled inside the casing with two separate chambers wherein flow arrangement of hot and cold fluid flow was done with two separate temperature controlled bath, as shown in Figure 2-c. Thermocouples were inserted at suitable locations in the inlet and outlet plenums to get the inlet and outlet temperatures of the heat transfer fluids. Two thermocouples were also placed on the central U-tubes of PHP (T_e and T_c), on both sides of the separator plate.

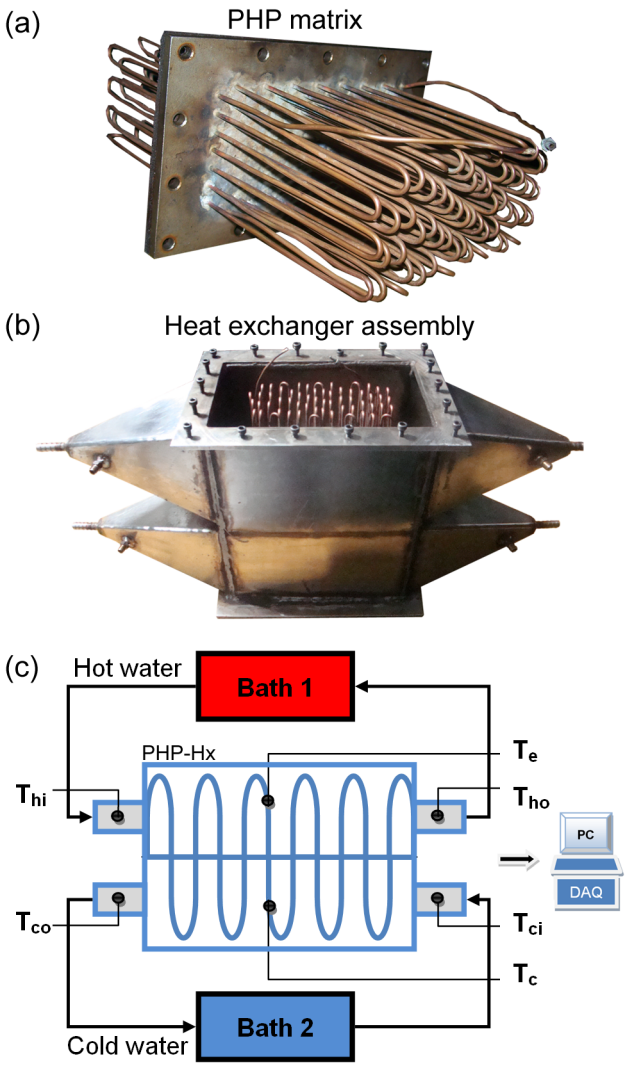

Figure 2. (a) PHP module (b) outer casing and coolant flow chambers (c) schematic of the complete setup.

NTU-Effectiveness formulation

In a conventional heat pipe/thermosyphon heat exchanger, heat is transferred between the high and low temperature fluids by evaporation and condensation of the heat pipe working fluid. With this configuration, the maximum heat capacity is due to the phase-change of the heat pipe working fluid. This fact leads to the analysis of the heat pipe heat exchangers as two separate heat exchangers coupled by the heat pipe working fluid, which is similar to a liquid-coupled indirect-transfer heat exchanger, as shown schematically in Figure 3-a,b. The equivalent heat exchanger system represented by Figure 3-b and the subsequent analysis is valid so far as the external heat transfer capacity of the heat exchanger system is an order of magnitude smaller than the internal heat capacity of the heat pipe (due to evaporation and condensation). In a conventional heat pipe, all the heat transfer is by latent heat transfer of the working fluid, PHP heat transport mechanism is a combination of latent and sensible heat, as noted earlier. While the exact percentage of latent heat and sensible heat transfer in a PHP is debatable and under scrutiny, it can still be safely said that internal heat transfer resistance is quite low. In this background, we explore the possibility of applying the effectiveness formulation for conventional heat pipe exchangers, as given by [Kays and London, 1984], to PHPs.

Effectiveness of any heat exchanger is defined as:

$$\varepsilon = \frac{\dot{Q}_{actual}}{\dot{Q}_{\max}} = \frac{C_h(T_{hi}-T_{ho})}{C_{\min}(T_{hi}-T_{ci})} = \frac{C_c(T_{co}-T_{ci})}{C_{\min}(T_{hi}-T_{ci})} \qquad (1)$$

Effectiveness of a typical counter flow heat exchanger is given as [Incropera and Dewitt, 1998]:

$$\varepsilon = \frac{1-\exp\left[-\frac{U_t S_t}{C_{\min}}\left(1-\frac{C_{\min}}{C_{\max}}\right)\right]}{1-\frac{C_{\min}}{C_{\max}}\exp\left[-\frac{U_t S_t}{C_{\min}}\left(1-\frac{C_{\min}}{C_{\max}}\right)\right]} \qquad (2)$$

where U_t and S_t are the overall heat transfer coefficient and heat transfer area on one side of heat exchanger. As the maximum heat capacity (in a heat pipe as well as a PHP) is several orders of magnitude larger than the minimum, due to phase change, $C_{min}/C_{max} \approx 0$, Eq. (2) is reduced to:

$$\varepsilon = 1-\exp(-NTU) \qquad (3)$$

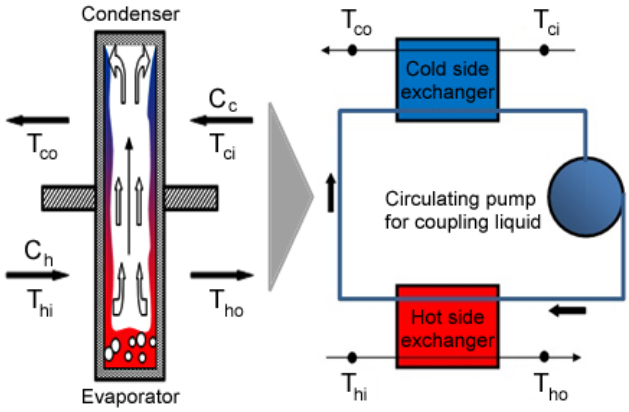

Figure 3. (a) Single heat pipe heat exchanger and, (b) its equivalent liquid-coupled indirect-transfer heat exchanger.

With reference to Figure 3-b, which shows the equivalent heat exchanger system representing the single heat pipe heat exchanger, the respective effectiveness values of the evaporator and condenser sections can thus be defined as:

$$\varepsilon_i = 1 - \exp(-NTU_i) \tag{4}$$

where,

$$NTU_i = \frac{U_i S_i}{C_i}: \quad i = h, c \tag{5}$$

The external heat transfer coefficient over the PHP tubes was modeled as single-phase external flow over a bank of staggered tubes. For staggered tube banks with 16 or more rows and $0<Re_{Do}<500$, $0.7<Pr<500$, average Nusselt number is given by [Incropera and Dewitt, 1998]:

$$Nu_{D_o} = 1.04 Re_{D_o}^{0.4} \cdot Pr^{0.36} \cdot \left(Pr / Pr_s\right)^{0.25} \tag{6}$$

In this correlation, all properties except Pr_s are to be evaluated at the arithmetic mean of the inlet and the outlet temperatures of the fluid and Pr_s is to evaluated at the surface temperature of tube (refer Figure 2-c: T_e and T_c). Here, D_o is taken as the outer diameter of the PHP tube and Re_{Do} is the local Reynolds number experienced by the staggered tube bank.

For an individual heat pipe, the effectiveness is defined as (Kays and London, 1984)

$$\varepsilon_{pipe} = \left(\frac{1}{\varepsilon_{\min}} + \frac{C^*}{\varepsilon_{\max}} \right)^{-1} \tag{7}$$

where ε_{min} and ε_{max} are the minimum and maximum values of ε_h and ε_c, respectively, from Eq. (4). The heat capacity ratio C^* is given by:

$$C^* = \frac{C_{\min}}{C_{\max}} \text{ such that } C^* \le 1.0 \tag{8}$$

where C_{max} is the larger of the heat capacities of the high and low temperature fluid streams and C_{min} is the smaller value, respectively.

For a single stage of heat pipes in the heat exchanger, S_h and S_c are based on the total heat transfer area in that stage. For a multi-stage heat pipe heat exchanger, in which there are a number of stages, each containing a column of heat pipes (normal to the high and low temperature fluid streams), the effectiveness can be determined by considering the columns of heat pipes as separate heat exchangers connected together in series, similar to that of a multi-pass heat exchanger. For such a multi-stage system in counter flow arrangement, the heat exchsnger effectiveness is given by [Kays and London, 1984]:

$$\varepsilon = \frac{\left(\frac{1 - C^* \varepsilon_p}{1 - \varepsilon_p} \right)^n - 1}{\left(\frac{1 - C^* \varepsilon_p}{1 - \varepsilon_p} \right)^n - C^*} \tag{9}$$

where n is the number of stages and C^* is defined by Eq. (8).

HEAT FLUX CONTROLLED MODULE

Experimental set-up

The details of the set-up are shown in Figure 4. The PHP module was formed by brazing a continuous copper capillary tube array (ID = 2.0 mm OD = 3.0 mm), shaped in serpentine U-shaped loops, on a copper base plate of size 100×100×4 mm^3. Net volume of PHP was 65±2 ml; working fluid was ethanol. In this array, there were 8 rows and every row had 14 pipe loops. Height of every loop was 92±1 mm. The PHP array was attached to a surface mountable flat heater and kept inside an air-flow control facility wherein the cooling air velocity was controlled. Average PHP heater block and base plate temperature were measured by four K-thermocouples; one thermocouple measured the inlet air temperature and two thermocouples measured the outlet temperature of the cooling air. The centerline air velocity in the flow facility was varied from 1 m/s to 6 m/s with ambient temperature of 25°C±1.5°C. Air velocity was recorded with a pre-calibrated hot wire sensor.

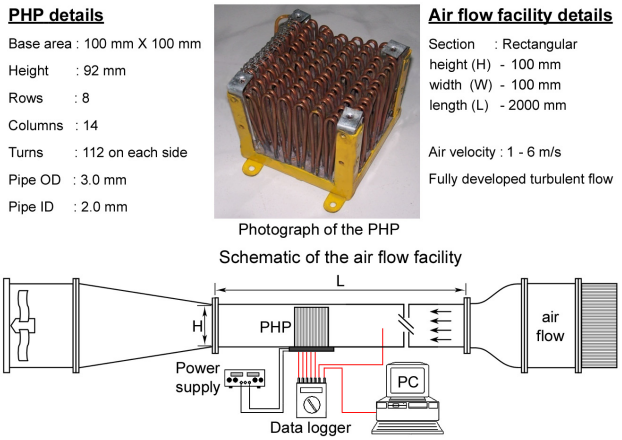

Figure 4. Details of the air-cooled PHP module.

Extended surface 'super-fin' formulation

One way of looking at this PHP module is from an 'extended surfaces' point of view. For example, the PHP tubes can be seen as fins protruding out of the evaporator block, as shown in Figure 5.

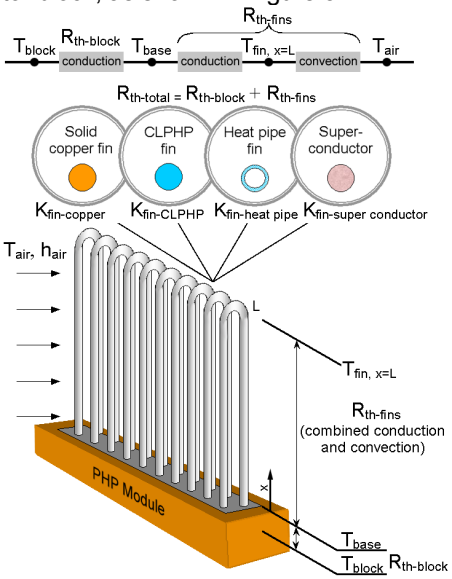

Figure 5. The 'super fin' analogy for modeling the heat transfer through a pulsating heat pipe.

The Biot number of the finned systems affects the longitudinal temperature distribution along the fin, which directly influences the resulting enhancement of heat transfer due to the fins. In the limit of infinite fin thermal conductivity ($Bi \rightarrow 0$), the entire fin would be at the base temperature, thereby providing maximum possible heat transfer rate. An ideal conventional heat pipe represents this case. In practice though, heat pipes also have a finite thermal resistance. With this viewpoint, referring to Figure 5, the essential question to answer is:

- What is the comparison between PHPs, in terms of thermal resistance and weight, and (a) an equivalent solid copper based fin system, and, (b) an equivalent conventional heat pipe fin system?

Typical weight ratio comparison of PHP tubes with solid copper rod is ~ 0.45.

Performance testing of conventional copper-water mini-heat pipes indicates that the maximum performance drastically reduces while the thermal resistance increases, with decreasing heat pipe diameter [Tang et al., 2004]. In addition, the manufacturing complexity of small diameter conventional capillary heat pipes also increases with decreasing tube diameter. The estimated k_{eff} (based on heat pipe OD) in vertical heater-down position, optimized for the range of operating temperatures tested (30°C to 80°C), is shown in Table 1. This provides an 'order of magnitude' indication to the designer of what is practically achievable by copper-water conventional cylindrical mini heat pipes.

Table 1. Effective thermal conductivity of mini heat pipes in vertical heater-down position [Tang et al., 2004]

ID/OD (mm)	$\dot{Q}_{max}$ at T_a=60°C (W)	R_{th} (K/W)	L_{eff} (mm)	A_{cs} (mm^2)	k_{eff} (W/mK)
3.0/4.0	27.0	0.3	210	12.56	55732
2.5/3.0	21.5	1.1	96	7.07	12344
2.0/2.5	16.0	3.25	85	4.91	5326

To find out the k_{eff} of the tested PHP, the air side heat transfer coefficient, i.e., h_{air} is needed. This is estimated from the dry PHP test (with no fluid inside; FR = 0%). By knowing the PHP tube geometry and experimentally obtaining T_{block}, T_{base}, T_{air} and $\dot{Q}_{fin}$, we can analyze this case by the standard one-dimensional conduction equation in extended surfaces, with convective boundary at the fin tip [Incropera and Dewitt, 1998], as:

$$\dot{Q}_{fin} = M \cdot \left(\frac{\sinh(mL) + (h_{air}/mk_{fin})\cosh(mL)}{\cosh(mL) + (h_{air}/mk_{fin})\sinh(mL)} \right) (T_{base} - T_{air}) \qquad (10)$$

$$\dot{Q}_{total} = (2N) \cdot \dot{Q}_{fin}, \text{ where,} \qquad (11)$$

$$M = \sqrt{h_{air} \cdot \hat{P} \cdot k_{fin} \cdot A_{cs}}; m = \sqrt{(h_{air} \cdot \hat{P})/(k_{fin} \cdot A_{cs})} \qquad (12)$$

$$A_{cs} = (\pi/4)\left(D_o^2 - D_i^2\right) \text{ and } \hat{P} = \pi D_o \qquad (13)$$

For a given cooling air velocity, the air side heat transfer coefficient (h_{air}) are applicable in the entire range of PHP experiments i.e. including those where the PHP is filled and is operating with a two-phase mixture inside the tube). With this known h_{air}, Eq. (10) can again be used to determine the $(k_{fin})_{eff}$ for all the cases of interest when the PHP is partially filled with the working fluid.

RESULTS AND DISCUSSION

Temperature controlled module

All experiments have been done with three different hot water inlet temperatures (60°C, 75°C and 80°C; all at fixed flow rate of 1.18 × 10^{-4} m^3/s) while the cold water inlet temperature was always kept constant at 35°C (flow rate = 1.6 × 10^{-5} m^3/s).

Figure 6 shows the typical temperature-time history for the PHP with FR = 40% and operating with gravity assisted bottom heating mode. Initially, up to point 'A', both T_{hi} and T_{ci} were kept at 35ºC. At point 'A', T_{hi} was set at 60ºC by the constant temperature bath. After sometime, when steady state was achieved at this temperature, T_{hi} was again set at 75ºC at 'B', followed by 85°C at point C. Maximum ambient heat losses were limited to 7-11%. In this case, the pulsating heat pipe starts operating even at the lowest hot water temperature of 60ºC, as is indicated by the oscillations observed in T_e and T_c. As T_{hi} increases, the PHP operation becomes more favorable and efficient.

Figure 7-a,b shows the comparison of net heat throughput for FR = 0% (dry system), 40%, 60% and 80% respectively, in gravity assisted mode and anti-gravity mode. Net heat throughput is maximum at FR = 40% as compared to other filling ratios in both the modes. In anti-gravity mode, the heat pipe heat exchanger starts working effectively only at T_{hi} = 85ºC. At lower heating temperatures, oscillations in working fluid temperature (T_e and T_c, refer Figures 2-c and 6) are not recorded; this indicates lesser internal fluid oscillations, thus explaining the lower heat throughput.

Figure 8 shows the comparison of heat exchanger effectiveness, as obtained by using Eq. (1)-(9), in gravity assisted orientation of the heat exchanger at different filling ratios. As can be seen, the effectiveness of the device increases with increasing hot water inlet temperature (temperature difference between the hot and the cold fluid). Maximum effectiveness of about 0.43 is achieved at the filling ratio of 40%. It is to be noted that no additional fining or surface area enhancement has been done on the exterior of the PHP tubes, i.e. the tubes are bare, as seen in Figure 2-a. With additional cross-fining, to increases the outside heat transfer area, effectiveness can certainly be enhanced further. Effectiveness diminishes with increasing filling ratio as the oscillating tendency of the fluid gets hampered.

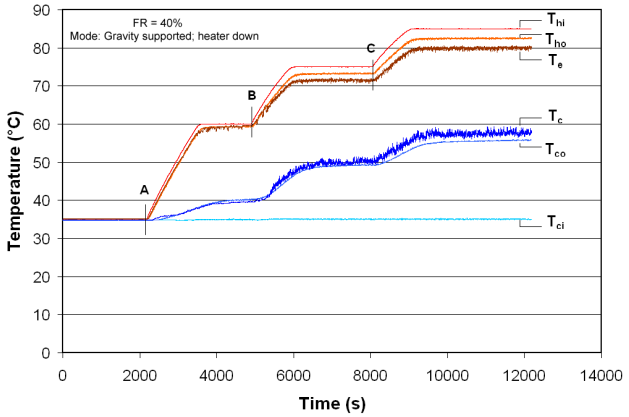

Figure 6. Typical temperature-time history of PHP-Hx at FR = 40% and gravity supported operation.

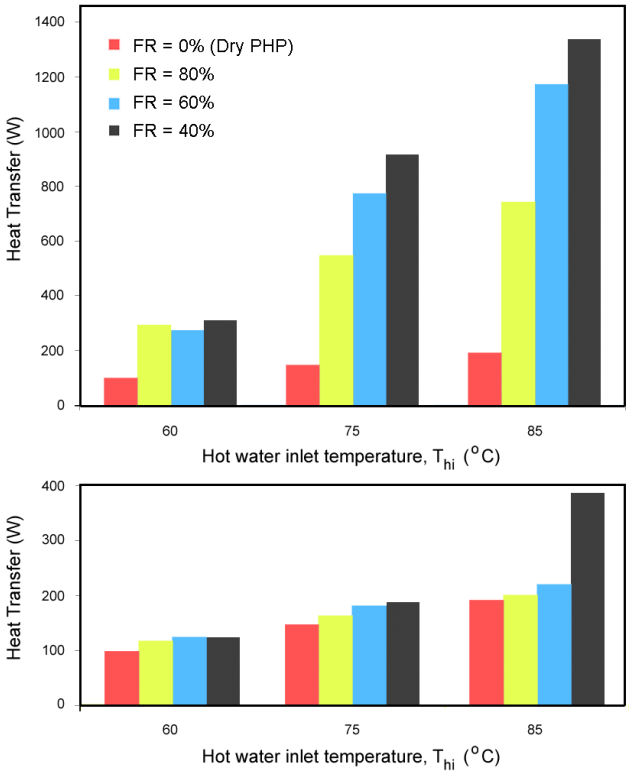

Figure 7. Comparison of heat throughput in (a) gravity supported orientation, and, (b) in Anti-Gravity orientation.

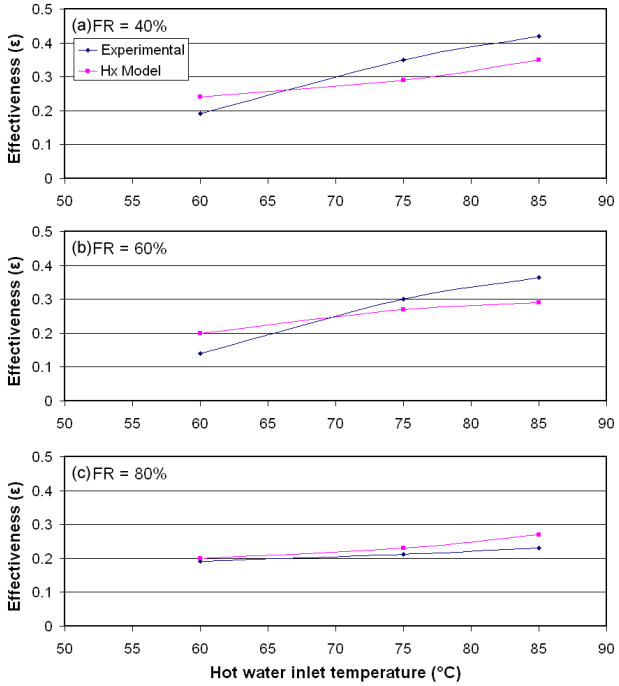

Figure 8. Comparison of experimental data with NTU-ε heat exchanger model in (a) Gravity assisted orientation, FR 40%, and, (b) FR 60% (c) FR 80%.

These preliminary results clearly indicate that the *NTU-ε* model for a conventional heat pipe is reasonably valid for the PHP, as the thermal capacity of the latter is still quite high, although not as high as a conventional heat pipe systems. More studies are needed to establish these working correlations for design purpose.

Heat flux controlled module

The average evaporator (T_{block}) and condenser (PHP tube tip) temperature ($T_{fin,\ x=L}$; refer Figure 5) during a typical power ramp-up test is as shown in Figure 9. The test was stopped when the average evaporator temperature reached about 100ºC. As can be seen, the module is able to handle about 800 W for this safe maximum evaporator temperature at centerline air velocity of 6 m/s.

At applied power levels below ~200W, the oscillations inside the device are not vigorous enough. As power levels are increased, increased oscillating tendencies drastically reduce the thermal resistance, defined as:

$$R_{th} = \left(T_{block} - T_{air}\right) / \dot{Q}_{total} \qquad (14)$$

The entire profile of thermal resistance for the PHP module is shown in Figure 10. At these high heat flux levels, the module successfully operates in both orientations, gravity supported as well as anti-gravity with comparable thermal resistance.

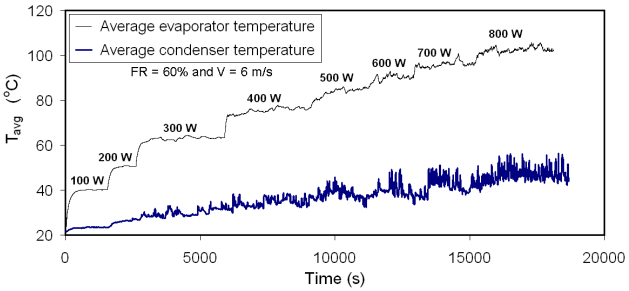

Figure 9. Temporal evolution of average evaporator and condenser temperatures at V = 6m/s.

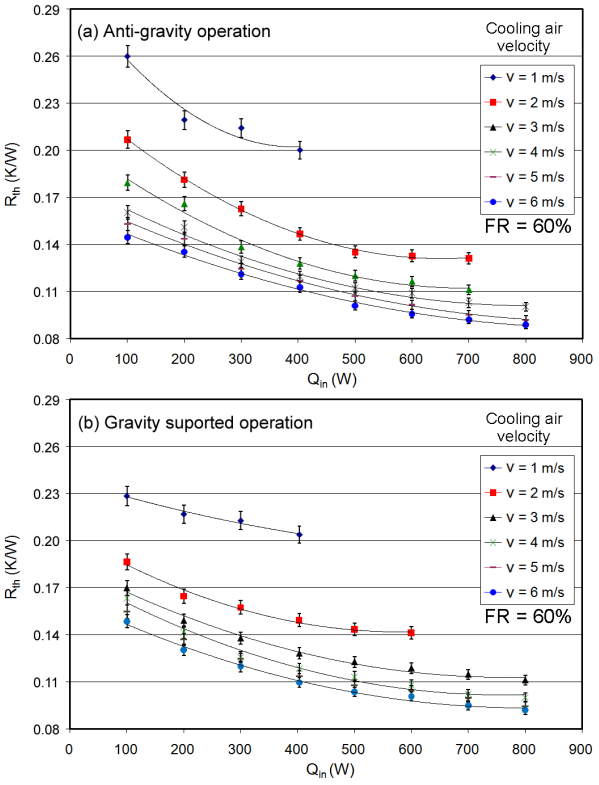

Figure 10. Variation of thermal resistance of the PHP module with heat input power (a) anti-gravity operation (b) gravity supported, heater down, operation.

The estimation of air side heat transfer coefficient (h_{air}), as discussed earlier, is shown in Figure 11. As expected, it increases in the range of 40 W/m^{2}K to 100 W/m^{2}K with increasing centerline air velocity from 1 m/s to 6 m/s. The scatter in the heat transfer coefficient data by repeating these tests was within ± 8 %.

After obtaining h_{air}, the effective thermal conductivity of the PHP module (k_{eff}) based on the PHP tube cross section can be estimated, as shown in Figure 12, for both orientations of the device operations. Comparing with Table 1, it is clear that PHPs are not as effective as conventional heat pipe, at least in the gravity assisted operation. Nevertheless, very high thermal conductivities are still achievable which are attractive, especially under situations when the net heat transfer is limited by external heat transfer coefficient, as in air cooling.

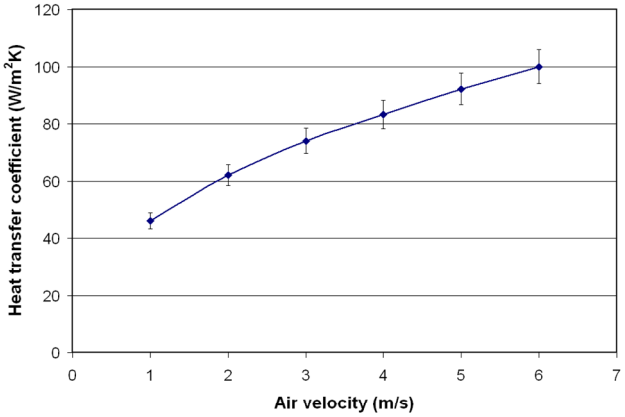

Figure 11. External cooling air side heat transfer coefficient vs. centre line velocity of cooling air.

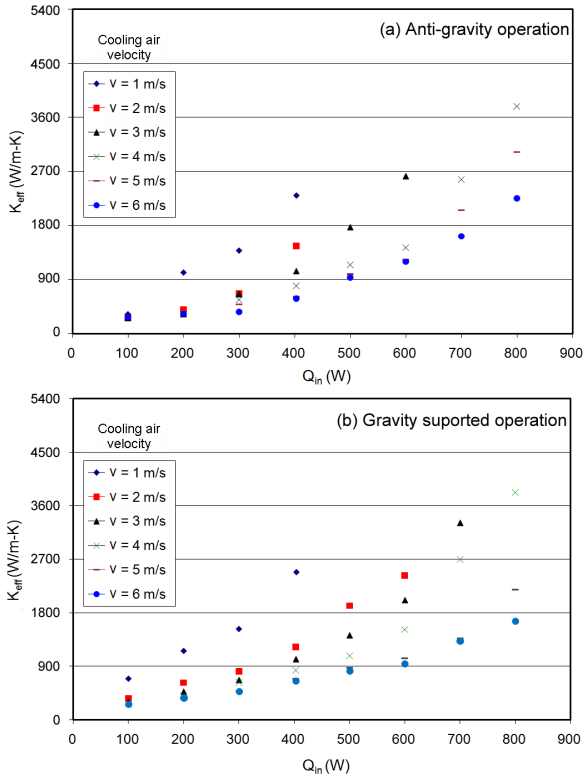

Figure 12. Effective thermal conductivity of the PHP (FR = 60%) as estimated from the fin analogy (a) anti-gravity operation (b) gravity supported, heater down, operation.

It is clear that the nature of the mixed conduction-convection heat transfer represented by Eq. (10) is such that the heat throughput gets limited by the external heat transfer coefficient after a certain value of the fin thermal conductivity is achieved. With the achieved effective thermal conductivity, the tested PHP nearly acted as a 'super fin' system. While in vertical heater-down position, the mini-heat pipes may give slight advantage over the PHPs, the fact that PHPs can operate with near equal performance level in all orientations make a very strong case in their favor. In addition, as compared to solid copper fins, there is a sizable weight advantage.

The fin analogy, as presented above, indeed has some obvious limitations. From Eq. (10), it is quite easy to know the effect of the length of solid fin or the air side external heat transfer coefficient on the net heat throughput for fin materials with constant thermal conductivity. These trends may not be extrapolated for the case of PHPs or for mini-heat pipes. In the case of PHPs, for a given heat throughput an increase in overall device length will amount to greater dissipative losses affecting its effective thermal conductivity, while for conventional mini heat pipes, the maximum performance till dry-out will decrease with an increase in length. Similarly, an increase in the external heat transfer coefficient may not always guarantee an increased performance of mini heat pipes. If a heat pipe is operating at a temperature T_1 with heat input of $\dot{Q}_1$, very close to the dryout power $\dot{Q}_{dry-1}$, under such operating conditions, if the condenser capacity is increased by either lowering the coolant temperature or increasing its flow rate, there is a risk of a dryout to occur (refer Figure 13). This will happen since the operating temperature drops to T_2, for which $\dot{Q}_1$ is too high. Although there is no well defined adiabatic operating temperature for PHPs, a similar trend regarding the effect of condenser capacity may occur since increasing the condenser capacity affects not only the thermophysical properties of the working fluid, but as a side effect, alters the slug-annular flow pattern transitions, thereby altering the final performance [Khandekar, 2004; Yang et al. 2009]. This aspect has to be addressed while practical designing and needs further understanding.

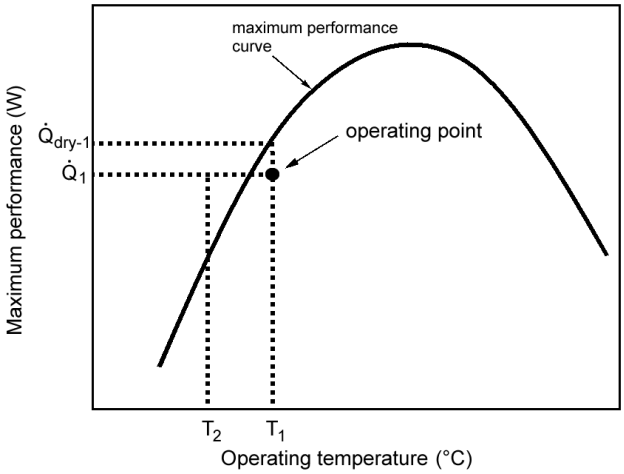

Figure 13. Dry-out in a conventional wicked heat pipe due to increase in condenser capacity.

SUMMARY AND CONCLUSIONS

We presented two types of PHP based heat exchangers (a) Temperature controlled liquid-liquid heat exchanger and, (b) Heat flux controlled air cooled module. Typical applications of such PHP heat exchangers may range from process waste heat recovery to high heat flux handling for power electronics applications. The primary transport mechanism of heat transfer along with the limitations in the present understanding of pulsating heat pipes was also briefly outlined.

The following conclusions can be drawn from the present study:

1. The effectiveness values for the temperature controlled heat exchanger system, operating under gravity assisted mode, were of the order of ~ 0.25-0.45; the heat exchanging PHP tubes being completely bare and un-finned. In anti gravity mode a higher temperature difference was needed to operate the system. In this module, FR = 40% gave better results as compared to FR = 60% and 80%.
2. The *NTU-ε* methodology of analysis for a conventional heat pipe heat exchanger is applicable for the PHP heat exchanger also. More systematic studies and data are required for further establishing this methodology of analysis for different PHP configurations and boundary conditions.
3. Heat flux controlled configuration is better suited for PHP applications. These devices can handle large heat fluxes. Effective thermal conductivities (k_{eff}) of the air cooled PHP module has been investigated by using extended surfaces fin analogy; k_{eff} values for the tested PHP are found to be of the order of 4-10 times that of pure copper. Effective thermal conductivity decreases with increasing heat flux.
4. Overall thermal resistances have been found to be very low (of the order of ~ 0.2 or lower), even though air cooling was employed. For a certain value of cooling air velocity, as the applied heat throughput increases, the value of overall thermal resistance decreases. The slopes of curves for thermal resistance vs. applied heat flux were initially found high, decreasing as the value of applied flux increases. For a given heat flux, as the cooling air velocity increases, the thermal resistance initially decreases faster and later levels off beyond ~ 3m/s.
5. For the low values of heat throughput, this air cooled PHP module performs better (in terms of thermal resistance and effective thermal conductivity) in gravity supported orientation than in anti-gravity orientation. As the applied heat flux increases, gravity does not play a significant role; comparable thermal resistances are obtained in both orientations. As compared to mini-cylindrical heat pipes, even if the effective thermal conductivity of PHPs is somewhat smaller, there is considerable advantage in the use of PHPs, especially in cases where external heat transfer coefficient limits the overall heat transfer and anti-gravity operation may occur. In addition, the fact that a PHP module operates equally well in all orientations is another major advantage.

NOMENCLATURE

A	Area (m^2)
C	Heat capacity (W/K)
C^*	Ratio of heat capacities (-)
C_p	Specific heat of fluid (J/kg-K)
D	Diameter (m)
F	Force (N)
g	Acceleration due to gravity (m/s^2)
h	Heat transfer coefficient (W/m^2-K)
k	Thermal conductivity (W/m-K)
L	Length (m)
M, m	Fin parameters, as per Eq. (12)
N	Number of U-turns on each side of a PHP (-)
n	Number of stages (-)
P	Pressure (N/m^2)
$\hat{P}$	Perimeter (m)
$\dot{Q}$	Heat throughput (W)
R_{th}	Thermal resistance (K/W)
S_t	Heat transfer area (m^2)
T	Temperature (°C)
U_t	Overall heat transfer coefficient (W/m^2-K)
V	Velocity (m/s)

Non-dimensional numbers

Bi	Biot number, $(h \cdot D) / k_{solid}$
Bo	Bond number, $D \cdot (g(\rho_{liq} - \rho_{vap}) / \sigma)^{0.5}$
NTU	Number of transfer units, $(U \cdot S) / C$
Nu	Nusselt number, $(h \cdot D) / k_{liq}$
Pr	Prandtl number, $(\mu_{liq} \cdot C_p) / k_{liq}$
Re	Reynolds number, $(\rho_{liq} \cdot V \cdot D) / \mu_{liq}$

Greek symbols

ε	Effectiveness (-)
μ	Dynamic viscosity (Pa·s)
ρ	Density (kg/m^3)
σ	Surface tension of the fluid (N/m)

Subscipts

av	average
c	cold fluid
ci, co	cold inlet, cold outlet
cs	cross-section
eff	effective
h	hot fluid
hi, ho	hot inlet, hot outlet
i	inner
liq	liquid phase
max	maximum
min	minimum
o	outer
s	surface
sat	saturation
vap	vapor phase

ACKNOWLEDGEMENTS

The work is supported by financial grants from Bhabha Atomic Research Center, Department of Atomic Energy, Government of India. Experimental work by Ashutosh Bhatnager, Vivek Silwal, Ankit Deepak Chowdhary and Shailendra Pal Veer Singh is also acknowledged.

REFERENCES

Akachi, H. (1996): US patent, Number 5490558.

Akachi, H., Polášek, F. and Štulc, P. (1996): "Pulsating Heat Pipes", Proc. 5th International Heat Pipe Symposium, pp. 208-217, Melbourne, Australia.

Angeli, P. and Gavriilidis, A. (2008): "Hydrodynamics of Taylor Flow in Small Channels: A Review", Proc. IMechE, Part C: J. Mechanical Engg. Sci., Vol. 222, pp. 737-751.

Das, S. P., Nikolayev, V. S., Lefevre, F., Pottier, B., Khandekar, S. and Bonjour J. (2010): "Thermally Induced Two-phase Oscillating Flow inside a Capillary Tube", International Journal of Heat and Mass Transfer, Vol. 53, pp. 3905-3913.

Groll, M., and Khandekar, S. (2003): "Pulsating Heat Pipes: Progress and Prospects", Proc. 3rd Int. Conf. on Energy and Environment", ISBN 7-5323-7335-5/TK-22, Vol. 1, pp. 723-730, Shanghai, China.

Incropera, F. P. and Dewitt, D. (1998): "Fundamentals of Heat and Mass Transfer", ISBN 0-471-30460-3, John Wiley & Sons.

Kays, W. M. and London, A.L. (1984): "Compact Heat Exchangers", McGraw-Hill, New York.

Khandekar, S. (2004): "Thermo-Hydrodynamics of Closed Loop Pulsating Heat Pipes", Doctoral dissertation, Universitaet Stuttgart, Germany, 2004 (available online at – http://elib.uni-stuttgart.de/opus/volltexte/2004/1939/

Khandekar, S., Dollinger, N. and Groll, M. (2003): "Understanding Operational Regimes of Pulsating Heat Pipes: An Experimental Study", Applied Thermal Engineering, Vol. 23, No. 6, pp. 707-719.

Tang, X., Hammel, E., Findl, W., Schmitt, T., Thumfart, D., Groll, M., Schneider, M. and Khandekar, S. (2004): "Study of AlSiC Metal Matrix Composite Based Flat Plate Thin Heat Pipe", Proc. 13th International Heat Pipe Conference, Shanghai, China.

Vasiliev, L. L. (2005): "Heat Pipes in Modern Heat Exchangers", Applied Thermal Engineering, Vol. 25, pp. 1-19.

Yang, H., Khandekar, S. and Groll M. (2009): "Performance Characteristics of Pulsating Heat Pipes as Integral Thermal Spreaders", International Journal of Thermal Sciences, Vol. 48 (4), pp. 815-824.

Zhang, H. and Faghri, A. (2008): "Advances and Unsolved Issues in Pulsating Heat Pipes", Heat Transfer Engineering, Vol. 29 (1), pp. 20-44.